ADVANCED MATERIALS

Supporting Information

for *Adv. Mater.*, DOI: 10.1002/adma.201802737

Control of Domain Structures in Multiferroic Thin Films through Defect Engineering

*Linze Li, Jacob R. Jokisaari, Yi Zhang, Xiaoxing Cheng, Xingxu Yan, Colin Heikes, Qiyin Lin, Chaitanya Gadre, Darrell G. Schlom, Long-Qing Chen, and Xiaoqing Pan**

Supporting Information

Control of domain structures in multiferroic thin films through defect engineering

*Linze Li, Jacob R. Jokisaari, Yi Zhang, Xiaoxing Cheng, Xingxu Yan, Colin Heikes, Qiyin Lin, Chaitanya Gadre, Darrel Schlom, Long-Qing Chen, and Xiaoqing Pan**

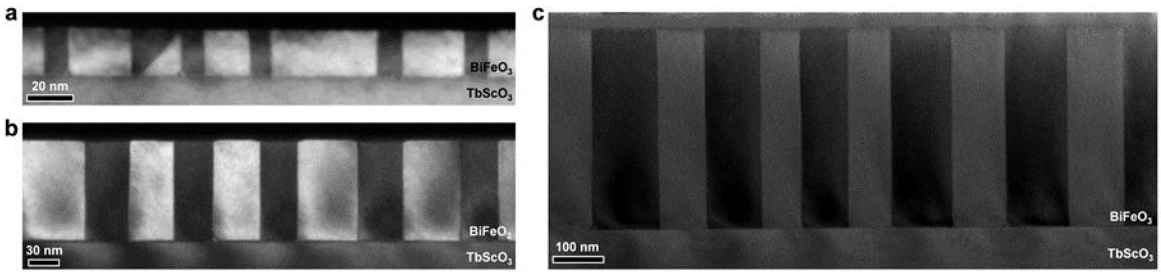

Figure S1. Dark-field diffraction-contrast TEM images of **a**, 20 nm, **b**, 100 nm, and **c**, 400nm $BiFeO_3$ thin films grown on $TbScO_3$ substrates, where impurity defects do not exist and regular 109° domain patterns are mostly observed in the films.

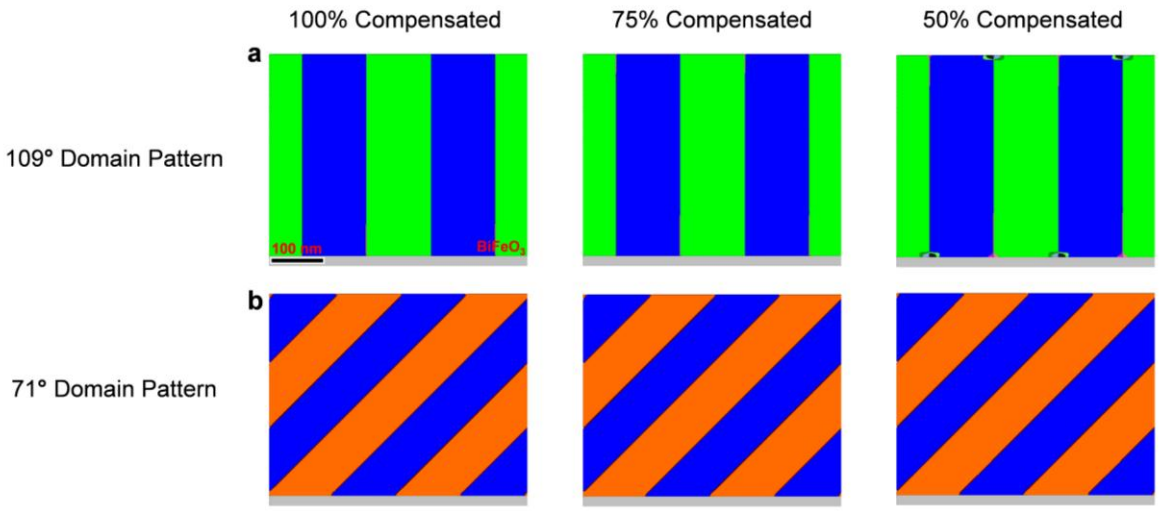

c

Energy Difference (E(109°) – E(71°))	Elastic	Electric	Landau	Gradient	Total
100%	3.82E+02	-1.69E+02	6.27E+02	7.72E+02	1.61E+03
75%	-6.63E+02	-2.86E+04	-7.94E+02	6.60E+02	-2.94E+04
50%	-3.71E+03	-3.43E+04	-5.40E+03	5.57E+02	-4.28E+04

Figure S2. a,**b**, 109° and 71° domain patterns calculated by phase-field simulations under different electrostatic boundary conditions (*i.e.*, the polarization bound charge at both interfaces are 100%, 75%, or 50% compensated). **c**, Calculated elastic, electric, landau, gradient, and total energy differences between 109° and 71°domain patterns. It is shown that when both interfaces are fully compensated (*i.e.*, 100% compensated), the 71° domain structure is more stable (*i.e.*, its total energy is lower). However, when the interfaces are partially compensated (75% or 50% compensated), which is more likely to be the real situation, the 109° domain structure is more stable. This is mainly due to the decreased electric energy of the 109° domain structure under partially compensated boundary conditions.

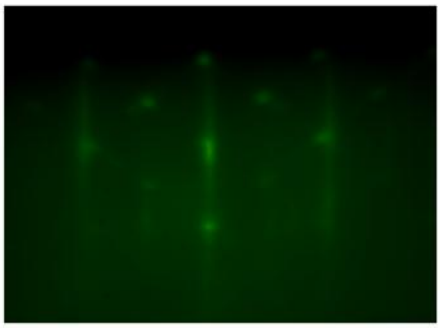

Figure S3. RHEED patterns collected during film growth. The streaks are associated with $BiFeO_3$ and the additional spots can be indexed to diffraction from (111)-oriented λ-Fe_2O_3.

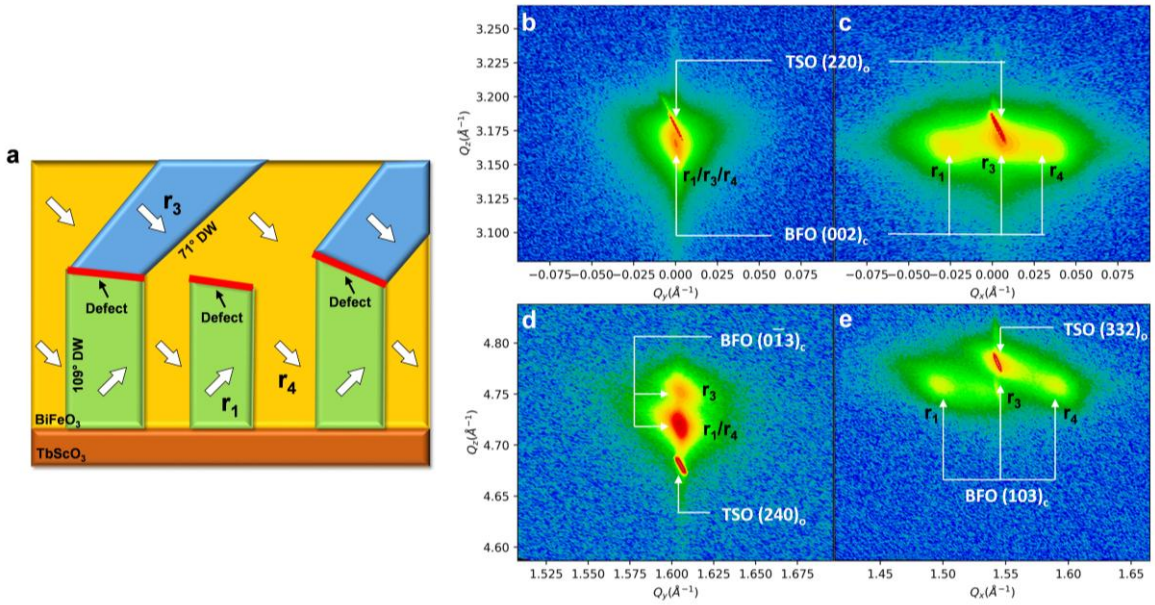

Figure S4. a, Schematic of polarization structures showing ordered 71° and 109° domains separated by an array of defects in the 400 nm $BiFeO_3$ film grown on $TbScO_3$ substrate. **b-e**, Reciprocal space map (RSM) analysis of this $BiFeO_3/TbScO_3$ heterostructure. **b**, Symmetric RSM result centered on TSO $(220)_o$ at φ= 0° where X-ray beam is along $[010]_c$. **c**, Symmetric RSM result centered on TSO $(220)_o$ at φ= 90° where X-ray beam is along $[100]_c$. **d**, Asymmetric RSM measurement centered on TSO $(240)_o$ at φ= 0°. **e**, Asymmetric RSM measurement centered on TSO $(332)_o$ at φ= 90°.

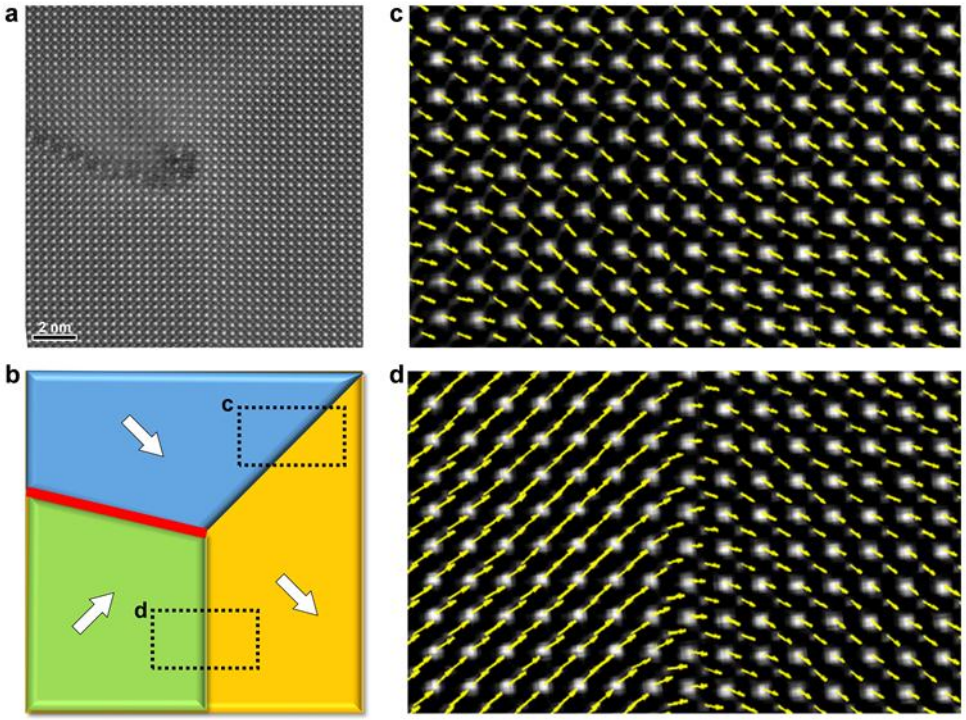

Figure S5. a, HAADF STEM image of a junction of 71° and 109° domain walls at the edge of a defect. **b**, The corresponding polarization configuration. **c**,**d**, Polarization mapping of the two regions highlighted in **b**. The polarization vectors are defined as the atomic displacement of the Fe cation from the center of the unit cell formed by its four Bi neighbors, which can be directly measured from the STEM HAADF images by fitting the atomic columns as two-dimensional (2D) Gaussian functions (see reference 17 for more information of this polarization mapping method).

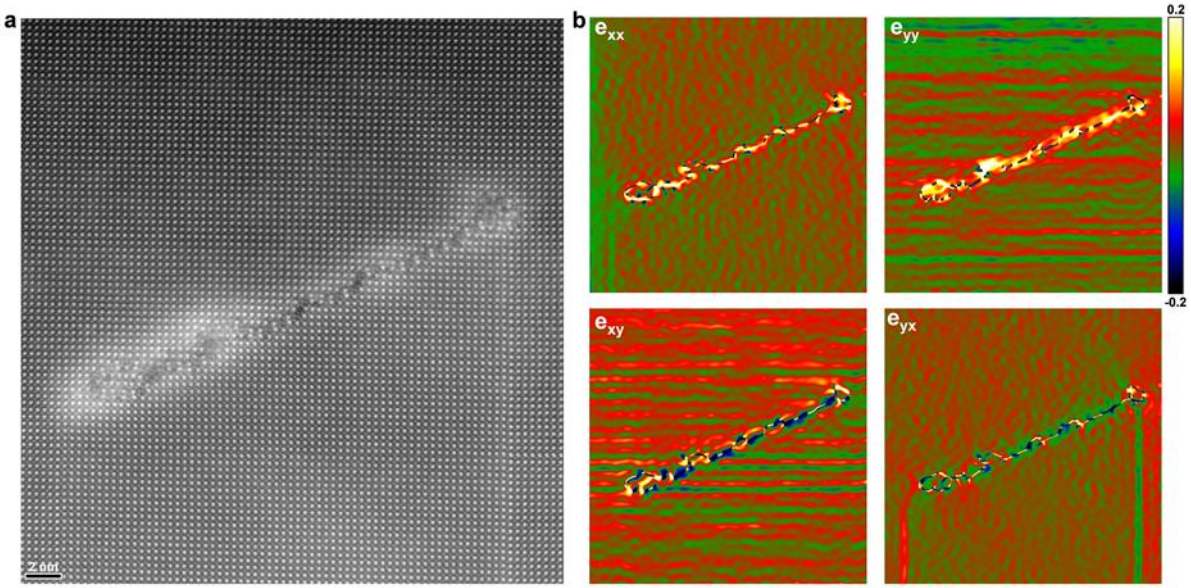

Figure S6. a, HAADF STEM image of a linear defect inserted in the $BiFeO_3$ matrix. **b**, Corresponding geometric phase analysis (GPA) of the HAADF STEM image revealing the strain in the $BiFeO_3$ lattice surrounding the defect. Note that the contrast at the defect is artifact due to the different structures of the $BiFeO_3$ matrix and the defect, and the striped patterns in e_{yy} and e_{xy} are caused by scanning noise in the STEM image.

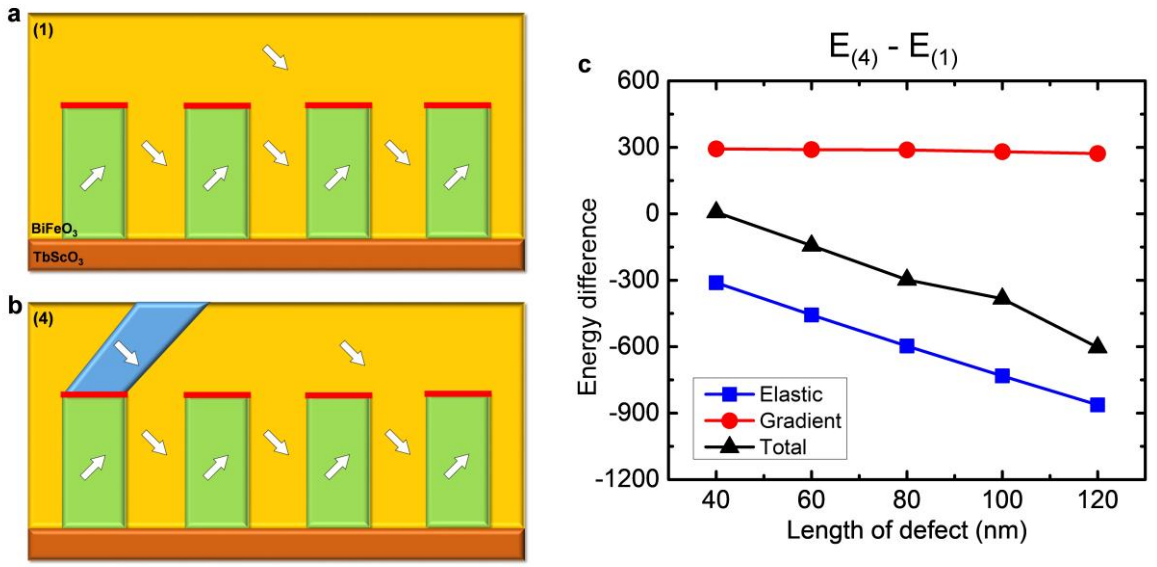

Figure S7. a,b, Schematics of two domain patterns modeled by phase-field simulations: (1) no 71° domains above the defect, and (4) one 71° domain on every four defects. The white arrows mark the polarization orientations. **c**, Calculated elastic, gradient, and total energy difference between these two domain patterns.

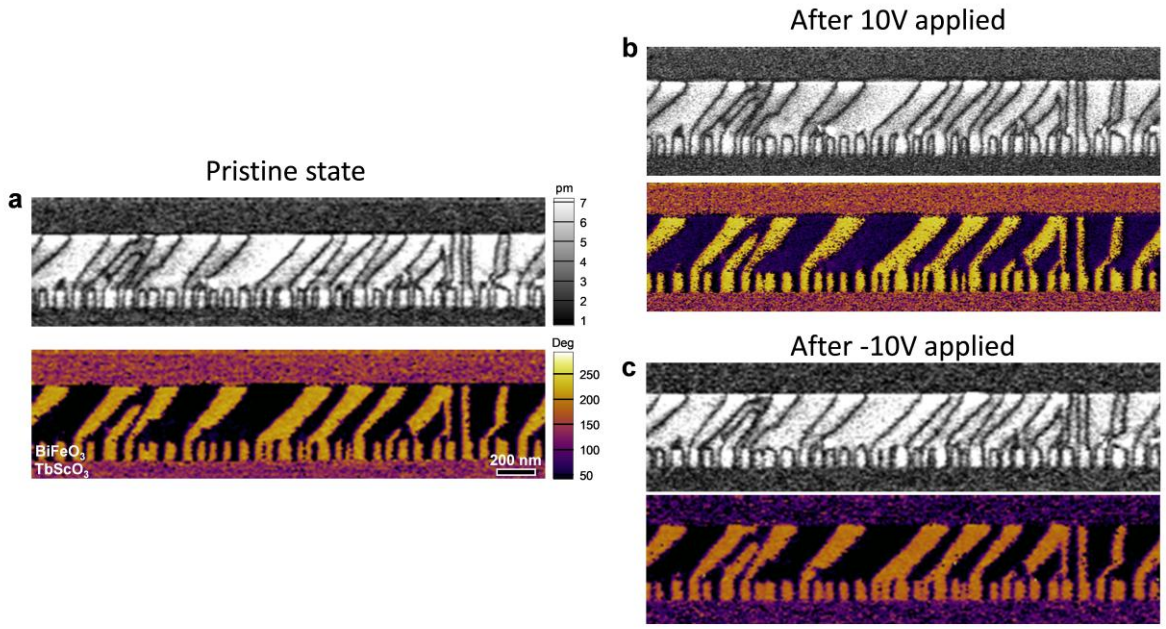

Figure S8. a, PFM amplitude (top) and phase (bottom) images of a region in the 400 nm $BiFeO_3$film containing ordered patterns of 71°domainsand 109° domains in the pristine state. **b**, PFM amplitude (top) and phase (bottom) images of the same region after a voltage of 10 V has been uniformly applied at the whole area with the scanning probe. **c**, PFM amplitude (top) and phase (bottom) images of the same region after a voltage of -10 V has been applied.